

Optimization of a Neutrino Factory: Discovery Machine versus Precision Instrument

Walter Winter

*Institut für theoretische Physik und Astrophysik, Universität Würzburg
Am Hubland, D-97074 Würzburg, Germany*

Abstract. We discuss the optimization of a neutrino factory experiment for the purpose of $\sin^2 2\theta_{13}$, mass hierarchy, and CP violation discoveries. This includes a review of possible optimization strategies, as well as an application of these to different $\sin^2 2\theta_{13}$ regions.

Keywords: Neutrino Oscillations, Neutrino Factory, Leptonic CP violation

PACS: 14.60.Pq

INTRODUCTION

The neutrino oscillation parameters are an important component to construct a theory for lepton masses and mixings. In lepton mass models, any observables describing deviations from potential symmetries turn out to be good performance indicators, which can be used to test the model parameter space. For example, the yet unknown value of $\sin^2 2\theta_{13}$ and the neutrino mass hierarchy are indicative for certain classes of models found in the literature, such as flavor symmetries or grand unified theories [1]. Similarly, deviations from maximal atmospheric mixing [2] may describe deviations from a ν_μ - ν_τ symmetry, and the phenomenological relationship $\theta_{12} + \theta_C \simeq \pi/4$ (“quark-lepton complementarity”) may be a performance indicator for quark-lepton unification [3]. In addition, there may be a connection between δ_{CP} and leptogenesis, which motivates the search for leptonic CP violation.

Three-flavor neutrino oscillations can be described by six parameters: The solar parameters Δm_{21}^2 and θ_{12} , the atmospheric parameters Δm_{31}^2 and θ_{23} , the small mixing angle θ_{13} , and the leptonic Dirac CP phase δ_{CP} . At this time, we know the solar and atmospheric oscillation parameters very well, but we do not know the sign of Δm_{31}^2 (neutrino mass hierarchy), the value of θ_{13} (we only have an upper bound for), and the leptonic CP phase (see, *e.g.*, Ref. [4]). In this talk, we therefore focus on the discoveries of (nonzero) $\sin^2 2\theta_{13}$, the neutrino mass hierarchy, and leptonic CP violation by means of a neutrino factory [5, 6, 7] producing neutrinos by muon decays in straight sections of a storage ring. The unprecedented reach and accuracy of a neutrino factory, and the broad scope of physics that can be explored has been discussed in detail in several studies (see, *e.g.*, Refs. [8, 9, 10, 11, 12, 13, 14, 15]). In particular, recently, the resolution of various degeneracies [12, 16, 17, 18] has

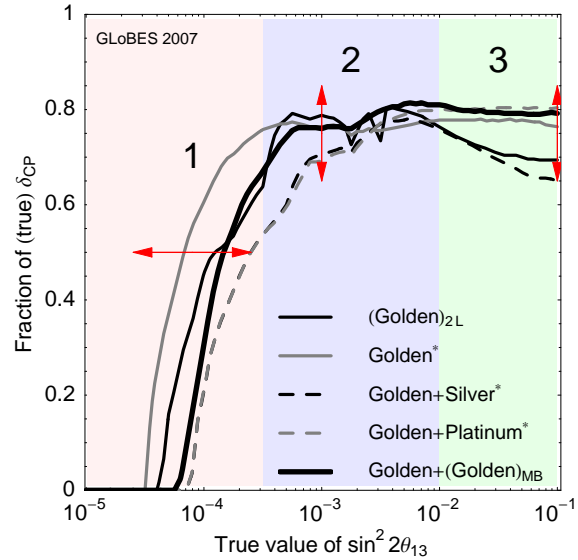


FIGURE 1. Fraction of δ_{CP} , for which CP violation can be discovered, as function of the true δ_{CP} for various different options (3σ). The three different optimization regions discussed in this talk are marked by different shadings and arrows. Similar figure as in Ref. [15].

been an important topic.

For the optimization of a neutrino factory, different $\sin^2 2\theta_{13}$ ranges are relevant which are illustrated in Figure 1 for the CP violation measurement. In this figure, we show the fraction of all possible (true) values of δ_{CP} for which one could establish CP violation as a function of the (true) $\sin^2 2\theta_{13}$. If we did not find $\sin^2 2\theta_{13} > 0$ in the next generation of experiments, it might be the primary objective to optimize for as small $\sin^2 2\theta_{13}$ as possible. For CP violation, that strategy is illustrated in the shaded

region 1 in Figure 1, where one would optimize along the respective arrow. This case is mainly limited by statistics and systematics. If, however, $\sin^2 2\theta_{13}$ turned out to be large, then one would optimize the fraction of δ_{CP} , for example, along the arrow in region 3. In this case, the main limitations are correlations among the oscillation parameters, such as with the matter density uncertainties (see, *e.g.*, Ref. [19]). In addition, the relatively high energy threshold above the interesting oscillation pattern affects the performance [14]. If, however, $\sin^2 2\theta_{13}$ was in region 2, one would optimize the fraction of δ_{CP} . In that region, discrete degeneracies limit the performance. Since the fraction of δ_{CP} for which one can measure CP violation is close connected to the precision of δ_{CP} at the CP conserving values, regions 2 and 3 correspond to an optimization of precision, whereas region 1 represents the discovery limit.

In this talk, we will discuss the optimization for regions 1, 2, and 3 separately. However, note that the next generation of experiments, such as superbeams and reactor experiments, will discover $\sin^2 2\theta_{13}$ only if $\sin^2 2\theta_{13} \gtrsim 0.01$ [20, 21]. In the discovery case, one will exactly know what $\sin^2 2\theta_{13}$ to optimize for. If on the other hand $\sin^2 2\theta_{13}$ is not discovered by these experiments, one will not know if $\sin^2 2\theta_{13}$ is in region 1 or 2. Therefore, if an decision has to be made at this point, a potentially contradictive optimization outcome between regions 1 and 2 will be very unfortunate. We will come back to this discussion in the conclusions.

OPTIMIZATION OPTIONS

Possible optimization options for a neutrino factory include the baseline(s), the muon energy, the combination of different oscillation channels, an optimization of the detector, or a potential luminosity increase¹. In addition, one could think of combinations with different experiment classes, such as superbeams [13, 22].

As potentially interesting appearance channels, we have the $\nu_e \rightarrow \nu_\tau$ (“silver”) [23, 24] and $\nu_\mu \rightarrow \nu_e$ (“platinum”) channels [25] in addition to the standard $\nu_e \rightarrow \nu_\mu$ (“golden”) channel [11, 12] using a magnetized iron calorimeter (MID).² For the silver channel, one typically assumes an OPERA-like emulsion cloud chamber (ECC) as a detector. Note that the silver channel requires relatively high muon energies because of the τ production threshold. In addition, one usually assumes that only the leptonic decay modes of the τ can be observed. For this talk, we will adopt the optimistic point of view that the hadronic decay modes can be observed as well, and that

one can built a 10kt detector called “Silver*”. For the platinum channel, the problem is that the produced electrons start producing showers very quickly, which makes charge identification at high energies practically impossible in an iron calorimeter. Again, we adopt the optimistic point of view that a detector technology without that problem can be found (such as liquid argon), and call the detector “Platinum*” (for details, see Ref. [15]). Note that the platinum channel is the T-inverted channel to the “golden” $\nu_e \rightarrow \nu_\mu$ channel. In principle, it allows for a CP violation measurement without having to disentangle the δ_{CP} effects from the matter effects (see, *e.g.*, Ref. [26]).

As for the detector optimization, a lower energy threshold may be achieved for the price of higher backgrounds [27]. This lower energy threshold would allow for lower muon energies because the energy range, where the main oscillation effects take place, can be covered with a better efficiency. For example, for very large $\sin^2 2\theta_{13}$, it allows for muon energies as low as $E_\mu \gtrsim 4\text{ GeV}$, and leads to a re-optimization of the baseline [22, 28, 29]. This relatively new idea will be referred to as a “low energy neutrino factory”. The corresponding detector with a lower threshold will be called “Golden*” in the following.

An interesting particular baseline option is the “magic baseline” (MB). It turns out that, two second order in $\sin 2\theta_{13}$ and $\alpha = \Delta m_{21}^2 / \Delta m_{31}^2$, the dependence on δ_{CP} disappears at this baseline $L \simeq 7500\text{ km}$ independent of the oscillation parameter values and neutrino energy [30]. This effect can be used for a degeneracy-free measurement of $\sin^2 2\theta_{13}$ and the mass hierarchy. The exact baseline depends on specifics of the matter density profile. However, in combination with a short baseline, the matter profile dependence is negligible as long as the second baseline is long enough ($7000\text{ km} \lesssim L \lesssim 9000\text{ km}$) [31].

In some cases, we will compare the results with the $\gamma = 350$ beta beam from Ref. [32], called “Beta beam” in the following.

OPTIMIZATION REGIONS

In the following, we discuss the optimization along the arrows in Figure 1 for the three different regions in that figure.

Region 1 (discovery for smallest $\sin^2 2\theta_{13}$): The simultaneous baseline and muon energy optimization was discussed in Ref. [15] (see also Refs. [9, 11, 12, 33]). For the resolution of degeneracies and the mass hierarchy measurement, the magic baseline turns out to be the best choice, and for the CP violation measurement, a shorter baseline in a relatively broad window $L \sim 2000 - 5000\text{ km}$. Therefore, the combination of these two baselines is the currently discussed baseline setup

¹ In the following, we will refer to double luminosity by “2L”.

² The different channels can also be operated with antineutrinos.

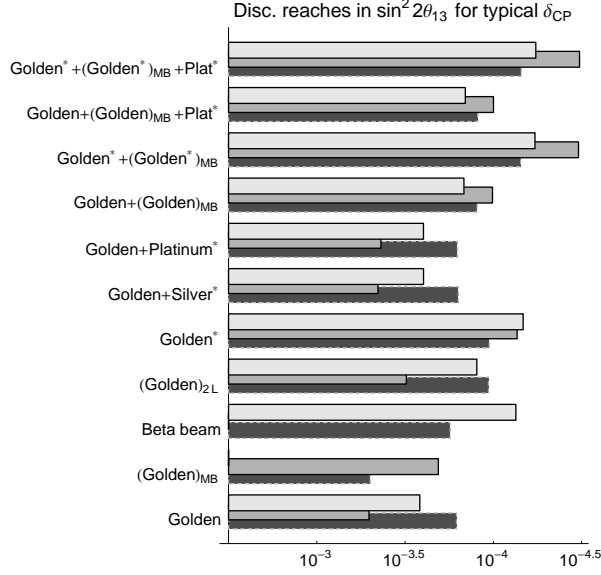


FIGURE 2. Comparison of options for CP violation (light bars, 3σ), mass hierarchy (medium gray bars, 3σ), and $\sin^2 2\theta_{13}$ discovery reaches (dark bars, 5σ). The figure shows the $\sin^2 2\theta_{13}$ reach for a CP fraction of 0.5 (“typical δ_{CP} ”). All bars Figure taken from Ref. [15].

of a neutrino factory [34]. Figure 2 summarizes the results for all three discovery reaches and for many different upgrade options. Note that the figure corresponds to the performance along the left arrow in Figure 1. From Figure 2, the magic baseline and the improved detection system are the key elements to improve the $\sin^2 2\theta_{13}$ reach. The Golden* detector allows for muon energies as low as $E_\mu \simeq 20 \text{ GeV}$ at the discovery limit without loss of physics potential [15].

Region 2 (precision for intermediate $\sin^2 2\theta_{13}$): A number of different optimization options in this case are compared in Figure 3, right panel. The conclusions are similar to the ones in region 1: magic baseline and improved detection system would clearly help. Compared to region 1, however, the $\sin^2 2\theta_{13}$ discovery turns out to be not a problem for almost any of the discussed options, and the discussion centers around the mass hierarchy and CP violation discoveries. One can also read off this figure that the silver and platinum channels do have some degeneracy resolution potential. This, however, does not lead to a substantial physics potential increase beyond the use of magic baseline or improved detector anymore. Note that the usefulness of the magic baseline as a risk minimizer can be also seen in the δ_{CP} [35] and $\sin^2 2\theta_{13}$ precision [31] measurements. For example, a δ_{CP} precision of about 10 degrees can be achieved (1σ) independent of the true δ_{CP} with a combination of two baselines. Such a precision comparable to the magnitude of the

Cabibbo angle can, for example, be motivated in quark-lepton complementarity based models [36].

Region 3 (precision for large $\sin^2 2\theta_{13}$): In this region, the value of $\sin^2 2\theta_{13}$ will be likely discovered soon, and the $\sin^2 2\theta_{13}$ discovery is not relevant for the optimization anymore. In addition, as one can see in Figure 3, left panel, the mass hierarchy can be easily determined for all possible values of δ_{CP} . Therefore, the optimization is determined by CP violation. In principle, there are two options for a neutrino factory discussed in the literature: A high energy option ($E_\mu \gtrsim 20 - 50 \text{ GeV}$), and a low energy option ($E_\mu \sim 5 \text{ GeV}$) if there are substantial improvements in the detection threshold (such as a different detector technology can be used).

Any optimization discussion of a neutrino factory for large $\sin^2 2\theta_{13}$ should take into account that there are competing experiments as well. For example, superbeam upgrades do have a similar physics potential and can be optimized, too (see, *e.g.*, Refs. [37, 38] for an optimization discussion of different options). In addition, several higher gamma beta beam options have been discussed in the literature [39, 40, 32, 41, 42], which may even be competitive for smaller $\sin^2 2\theta_{13}$. Therefore, we will use several representatives of these experiment classes for comparison.

For the optimization of the high neutrino energy option, several possibilities are summarized in Figure 3, left panel. In addition to magic baseline and improved detector, the platinum channel helps in this region. However, the $\gamma = 350$ beta beam shown for comparison has a very competitive physics reach. This comparison, of course, depends on the useful parent decays of the two different experiment classes, which are very difficult to compare until there are dedicated cost studies for both options. In addition to the possibilities discussed in Figure 3, improved knowledge on the matter density profile helps for large $\sin^2 2\theta_{13}$. However, if different channels and baselines are combined, this knowledge becomes obsolete [15], and, in fact, one can measure the average lower mantle density of the Earth at the level of 0.5% (1σ) with the very long baseline [31, 43, 44].

If the detection system can be improved and effort (in terms of muon energy) matters, the muon energy can be significantly reduced [22, 28, 29]. Several low energy neutrino factory options, as well as their optimization have been discussed in Ref. [22]. In particular, it may be an option to combine a neutrino factory with a superbeam directed to the same detector at the same baseline, which we call neutrino factory superbeam (NF-SB) [22]. This superbeam may even be produced in the same decay chain as the neutrino factory beam, or it may be produced by using two targets. A schematics for such an experiment can be found in Figure 4. The main idea is to have a platinum-like $\nu_\mu \rightarrow \nu_e$ channel with a spectrum shifted towards lower neutrino energies compared

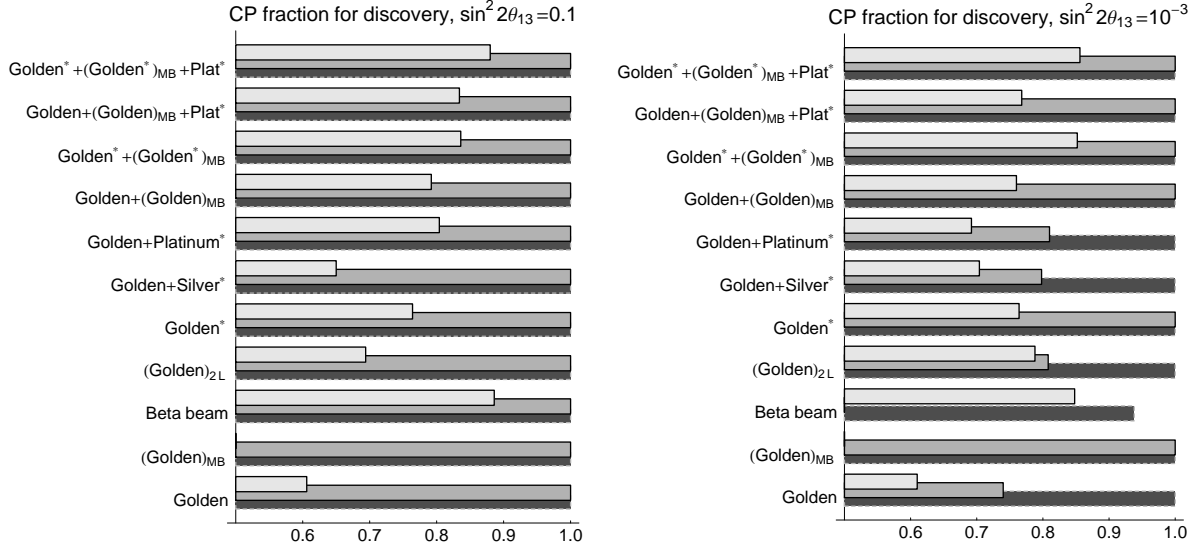


FIGURE 3. Comparison of options for CP violation (light bars, 3σ), mass hierarchy (medium gray bars, 3σ), and $\sin^2 2\theta_{13}$ discovery reaches (dark bars, 5σ). The figures show the fraction of δ_{CP} (“CP fraction”) for a given true $\sin^2 2\theta_{13}$ (see figure captions). Figure taken from Ref. [15].

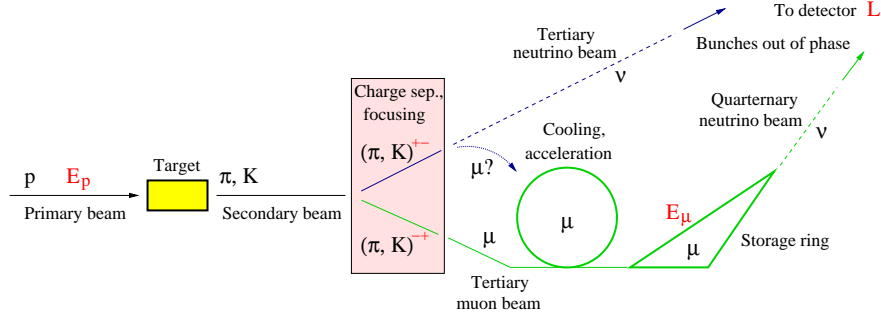


FIGURE 4. Schematics of a NF-SB (not to scale). Our degrees of freedom are given by red/gray labels. Note that we adopt the conservative point of view that only half the muons can be collected for the NF. Figure from Ref. [22].

to the platinum spectrum (the platinum spectrum is always peaking at higher energies compared to the golden channel because of the muon decay kinematics). In addition, out-of-phase bunches will not require charge identification of electrons at the detector. Since the interesting oscillation pattern tends to appear at lower energies, the absolute performance of a NF-SB is better than for a neutrino factory – even if the double luminosity is assumed for the neutrino factory alone (or only half of the muons can be collected for the neutrino factory mode). The optimal baseline is about 800 to 1500 km with $E_\mu \gtrsim 5$ GeV and $E_{\text{Prot}} = 28$ GeV. The NF-SB shows a very competitive behavior in the whole range $0.01 \lesssim \sin^2 2\theta_{13} \lesssim 0.1$, such as compared to a wide band superbeam upgrade using a megaton-size water Cherenkov detector. A similar result could be achieved for a low energy neutrino factory in combination with the platinum channel. That option,

however, requires electron charge identification.

SUMMARY AND CONCLUSIONS

In the previous discussion, we have optimized the different $\sin^2 2\theta_{13}$ regions for $\sin^2 2\theta_{13} \lesssim 0.01$ separately (*cf.*, Figure 1), because they correspond to different optimization goals: maximum reach in $\sin^2 2\theta_{13}$ (discovery limit) versus maximal reach in δ_{CP} (need for precision). However, it has turned out that the regions 1 and 2 have the same requirements: an improved detection system and a second (very long) baseline turn out to be key components of an optimized neutrino factory for $\sin^2 2\theta_{13} \lesssim 0.01$. Since we will, most likely, not know how big $\sin^2 2\theta_{13}$ is when we have to make a decision for region 1 or 2, the similar optimization outcome turns

out to be very fortunate.

If $\sin^2 2\theta_{13} \gtrsim 0.01$, we will have established a nonzero $\sin^2 2\theta_{13}$ very soon by the planned reactor and super-beam experiments. In this case, there are two options for a neutrino factory which are very different from the experimental point of view: They require different muon energies, different baselines, and, most importantly, a different detector. As for the combination with different channels, it remains to be clarified how well the platinum channel (electron neutrino detection with charge identification) can be implemented, and up to which energies. In sorting out the different options, the detector optimization and the test of different detector technologies are the key ingredients, and it should be one of the primary objectives for the coming years.

In this study, we have only focused on the optimization for the unknown neutrino oscillation parameters. However, different requirements, such as the search for non-standard physics or sensitivity to deviations from maximal atmospheric mixing, may lead to different optimizations. In the future, one will need to study how these different objectives fit together, and if there are any other unexplored experimental approaches.

Acknowledgments I would like to acknowledge support from the Emmy Noether program of Deutsche Forschungsgemeinschaft.

REFERENCES

1. C. H. Albright, and M.-C. Chen, *Phys. Rev. D* **74**, 113006 (2006), hep-ph/0608137.
2. S. Antusch, P. Huber, J. Kersten, T. Schwetz, and W. Winter, *Phys. Rev. D* **70**, 097302 (2004), hep-ph/0404268.
3. A. Y. Smirnov (2004), hep-ph/0402264.
4. T. Schwetz, *Phys. Scripta* **T127**, 1–5 (2006), hep-ph/0606060.
5. S. Geer, *Phys. Rev. D* **57**, 6989–6997 (1998), hep-ph/9712290.
6. C. Albright, et al., *Nucl. Phys. B* **547**, 21–38 (2000), hep-ex/0008064.
7. M. Apollonio, et al. (2002), hep-ph/0210192.
8. V. D. Barger, S. Geer, R. Raja, and K. Whisnant, *Phys. Rev. D* **62**, 013004 (2000), hep-ph/9911524.
9. V. Barger, S. Geer, and K. Whisnant, *Phys. Rev. D* **61**, 053004 (2000), hep-ph/9906487.
10. V. D. Barger, S. Geer, R. Raja, and K. Whisnant, *Phys. Lett. B* **485**, 379–387 (2000), hep-ph/0004208.
11. A. Cervera, et al., *Nucl. Phys. B* **579**, 17–55 (2000), hep-ph/0002108.
12. J. Burguet-Castell, M. B. Gavela, J. J. Gomez-Cadenas, P. Hernandez, and O. Mena, *Nucl. Phys. B* **608**, 301–318 (2001), hep-ph/0103258.
13. J. Burguet-Castell, M. B. Gavela, J. J. Gomez-Cadenas, P. Hernandez, and O. Mena, *Nucl. Phys. B* **646**, 301–320 (2002), hep-ph/0207080.
14. P. Huber, M. Lindner, and W. Winter, *Nucl. Phys. B* **645**, 3–48 (2002), hep-ph/0204352.
15. P. Huber, M. Lindner, M. Rolinec, and W. Winter, *Phys. Rev. D* **74**, 073003 (2006), hep-ph/0606119.
16. G. L. Fogli, and E. Lisi, *Phys. Rev. D* **54**, 3667–3670 (1996), hep-ph/9604415.
17. H. Minakata, and H. Nunokawa, *JHEP* **10**, 001 (2001), hep-ph/0108085.
18. V. Barger, D. Marfatia, and K. Whisnant, *Phys. Rev. D* **65**, 073023 (2002), hep-ph/0112119.
19. T. Ohlsson, and W. Winter, *Phys. Rev. D* **68**, 073007 (2003), hep-ph/0307178.
20. P. Huber, M. Lindner, M. Rolinec, T. Schwetz, and W. Winter, *Phys. Rev. D* **70**, 073014 (2004), hep-ph/0403068.
21. M. G. Albrow, et al. (2005), hep-ex/0509019.
22. P. Huber, and W. Winter, *Phys. Lett. B* (to be published), arXiv:0706.2862 [hep-ph].
23. A. Donini, D. Meloni, and P. Migliozzi, *Nucl. Phys. B* **646**, 321–349 (2002), hep-ph/0206034.
24. D. Autiero, et al. (2003), hep-ph/0305185.
25. A. Bueno, M. Campanelli, S. Navas-Concha, and A. Rubbia, *Nucl. Phys. B* **631**, 239–284 (2002), hep-ph/0112297.
26. E. K. Akhmedov, R. Johansson, M. Lindner, T. Ohlsson, and T. Schwetz, *JHEP* **04**, 078 (2004), hep-ph/0402175.
27. A. Cervera, MIND, A magnetized iron detector (2007), talk given at Golden 07.
28. S. Geer, O. Mena, and S. Pascoli, *Phys. Rev. D* **75**, 093001 (2007), hep-ph/0701258.
29. A. D. Bross, M. Ellis, S. Geer, O. Mena, and S. Pascoli (2007), arXiv:0709.3889 [hep-ph].
30. P. Huber, and W. Winter, *Phys. Rev. D* **68**, 037301 (2003), hep-ph/0301257.
31. R. Gandhi, and W. Winter, *Phys. Rev. D* **75**, 053002 (2007), hep-ph/0612158.
32. J. Burguet-Castell, D. Casper, E. Couce, J. J. Gomez-Cadenas, and P. Hernandez, *Nucl. Phys. B* **725**, 306–326 (2005), hep-ph/0503021.
33. M. Freund, P. Huber, and M. Lindner, *Nucl. Phys. B* **615**, 331–357 (2001), hep-ph/0105071.
34. S. King et al. (eds), Physics at a future neutrino factory and superbeam facility (to appear), ISS Physics working group report.
35. P. Huber, M. Lindner, and W. Winter, *JHEP* **05**, 020 (2005), hep-ph/0412199.
36. W. Winter (2007), arXiv:0709.2163 [hep-ph].
37. V. Barger, P. Huber, D. Marfatia, and W. Winter, *Phys. Rev. D* **76**, 031301 (2007), hep-ph/0610301.
38. V. Barger, P. Huber, D. Marfatia, and W. Winter, *Phys. Rev. D* **76**, 053005 (2007), hep-ph/0703029.
39. J. Burguet-Castell, D. Casper, J. J. Gomez-Cadenas, P. Hernandez, and F. Sanchez, *Nucl. Phys. B* **695**, 217–240 (2004), hep-ph/0312068.
40. P. Huber, M. Lindner, M. Rolinec, and W. Winter, *Phys. Rev. D* **73**, 053002 (2006), hep-ph/0506237.
41. S. K. Agarwalla, S. Choubey, and A. Raychaudhuri, *Nucl. Phys. B* **771**, 1–27 (2007), hep-ph/0610333.
42. S. K. Agarwalla, S. Choubey, and A. Raychaudhuri (2007), arXiv:0707.3367 [hep-ph].
43. W. Winter, *Phys. Rev. D* **72**, 037302 (2005), hep-ph/0502097.
44. H. Minakata, and S. Uchinami, *Phys. Rev. D* **75**, 073013 (2007), hep-ph/0612002.